TRANSACTIONS ON ELECTRICAL AND ELECTRONIC MATERIALS
Vol. 17, No. 4, pp. 208-211, August 25, 2016

Regular Paper

pISSN: 1229-7607 eISSN: 2092-7592
DOI: http://dx.doi.org/10.4313/TEEM.2016.17.4.208
OAK Central: http://central.oak.go.kr

Variations of the Thermoelectric Characteristics of ZnO Nanofibers from the Use of a Thermal Treatment

Yoonbeom Park, Kyoungah Cho[†a], Donghoon Lee, and Sangsig Kim[†b]
Department of Electrical Engineering, Korea University, Seoul 02841, Korea

Received May 18, 2016; Revised June 7, 2016; Accepted June 11, 2016

In this study, thermal-treatment-derived variations of the thermoelectric characteristics of ZnO nanofibers (NFs) are examined. NFs that were prepared by electrospinning were transformed into n-type ZnO NFs after they were exposed to thermal heating for 30 min at 550℃. For the ZnO NFs, the Seebeck coefficient decreased from - 132.1 μV/K to - 44.6 μV/K over the heating-time range of 30 min to 120 min, while the electrical conductivity increased from 2.07×10^{-3} S/m to 0.18 S/m.

Keywords: ZnO, Thermoelectric, Sintering

1. INTRODUCTION

Recently, oxide nanofibers (NFs) have attracted considerable attention as environmentally friendly thermoelectric materials that are distinct from the conventional thermoelectric materials including bismuth-telluride compounds [1-4]. In relation to the conventional thermoelectric nanomaterials, the advantages of the oxide NFs are derived from sufficient length dimensions that enable real-life oxide-NF applications [5-7]. Most NFs have been prepared with electrospinning and a subsequent thermal treatment, the latter of which affects the NF diameter and the residual-polymer quantity. Over time, heating-temperature and cooling-rate adjustments have been attempted to form oxide NFs with high thermoelectric efficiencies [7,8]; nevertheless, a dearth of studies regarding the effect of the heating time on the thermoelectric characteristics exists.

In terms of the fabrication of thermoelectric modules that are composed of *n*-type and *p*-type NF couples, *n*-type oxide NFs are important; however, a paucity of studies regarding the *n*-type oxide NFs presently exists, while the *p*-type oxide NFs including *p*-type $Ca_3Co_4O_9$ and *p*-type $LaSrCoO_3$ have been widely researched [6-10]. In this study, *n*-type ZnO thermoelectric NFs are therefore prepared, and the heating-time-based variations of the thermoelectric characteristics of these ZnO NFs are examined.

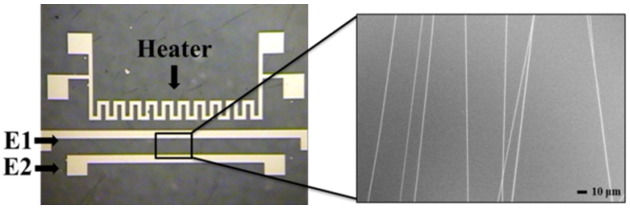

Fig. 1. Optical images of a thermoelectric platform that is constructed from a heater, two electrodes (E1 and E2), and ZnO NFs. The SEM image on the right side of the figure shows the ZnO NFs that are bridged between the E1 and the E2.

To investigate the in-air thermoelectric characteristics at room temperature, the ZnO NFs were fabricated on a platform that was constructed with a heater and two electrodes (E1 and E2) on a quartz substrate; the optical image of the thermoelectric platform is shown on the left side of Fig. 1. The SEM image on the right side of Fig. 1 demonstrates that the ZnO NFs are bridged between the E1 and the E2. The effect of the heating time on the thermoelectric characteristics of the ZnO NFs is examined according to thermal and structural analyses.

[†] Author to whom all correspondence should be addressed:
E-mail: [a]: chochem@korea.ac.kr, [b]: sangsig@korea.ac.kr

2. EXPERIMENTAL PROCEDURES

For the electrospinning of the NFs, a precursor solution was prepared through the mixing of zinc-acetate dihydrate, polyvinyl pyrrolidone (Mw = 1,300,000), ethanol, and distilled water [7]. On the fabricated thermoelectric platform, the separation between the E1 and the E2 is 160 μm, and a heater was located 40 μm away from the E1. With the use of a tungsten target, the heater and the electrodes were formed with sputtering; then, the thermoelectric platform was placed between two collectors for the electrospinning, and the precursor solution was loaded into a syringe that was equipped with a 0.25 mm-diameter needle that was connected to an 8 kV-power supply. The syringe was continuously supplied by a syringe pump at a rate of 0.5 μl/min. The as-electrospun NFs that collected on the platform were dried at 150℃ for 60 min on a hot plate, before they were thermally heated at 550℃ in a conventional furnace and under a nitrogen atmosphere for heating times that range from 10 min to 2 h.

The structural and thermal characteristics of the ZnO NFs were examined using X-ray diffraction (XRD, SmartLab), high-resolution transmission electron microscopy (HR-TEM, Tecnai-F20), SEM (JSM 7600F), and a thermogravimetric-differential thermal analyzer (TG-DTA, Exstar 6000). With the use of a semiconductor-parameter analyzer (HP4155C) and an infrared camera (FLIR A645SC) with a sensitivity of 30 mK and an uncertainty of 1%, the thermoelectric characteristics were then measured in air at room temperature.

The as-electrospun NFs (made of the zinc-acetate dehydrate and the polyvinyl pyrrolidone) were heated initially for 10 min as the temperature increased from room temperature to 550℃, and a subsequent heating at 550℃ occurred for 140 min. The TG and DTA curves that were then taken from the NFs under this thermal treatment are plotted in Fig. 2(a) as a function of the heating time; for clarity, the temperatures that were raised during the heating time are included in this figure.

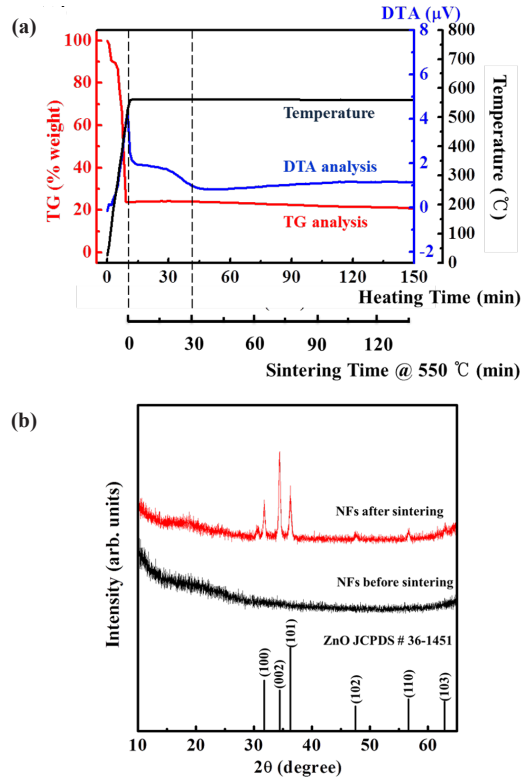

Fig. 2. (a) TG-DTA curve of NFs and (b) XRD patterns of ZnO NFs before and after sintering at 550℃ and JCPDS of ZnO (No. 36-1451).

3. RESULTS AND DISCUSSION

The TG analysis reveals that the weight of the NFs was dramatically reduced as the temperature was increased to 550℃ during the initial heating time. This dramatic reduction implies rapid decompositions of the zinc-acetate dehydrate and the polyvinyl-pyrrolidone side chains in the NFs. The TG curve also shows that the decomposition still progressed gradually for the subsequent heating time. The DTA curve in Fig. 2(a) demonstrates the three instances of exothermic progress for the combustion from the oxidation of the zinc-acetate dehydrate and the main chains of the polyvinyl pyrrolidone in the NFs. The second instance of the intra-NF exothermic progress that occurred during the subsequent heating time of 30 min at 550℃ is responsible for the synthesis and the sintering of the ZnO grains [11]. A gradual exothermic progress is present in the DTA curve for the subsequent heating time from 30 min to 140 min. This third instance of the exothermic progress indicates that the combustion of the organic remnants still occurs gradually in the NFs even after the synthesis of the ZnO grains.

The combustion aids the sintering of the ZnO grains; therefore, the TG and DTA analyses suggest that the synthesis and sintering of the ZnO grains occurs during the subsequent heating time. To avoid confusion, the subsequent heating time is named "sintering time" and is marked on the secondary x-axis in Fig. 2(a).

The XRD pattern for the NFs that were sintered for 30 min at 550℃ shows that these NFs are composed of ZnO materials. In Fig. 2(b), the XRD-pattern peaks are matched with the indexes of a wurtzite-lattice structure (ZnO JCPDS card no. 36-1451) that is of a (002)-preferred orientation [11]. The sharpness of the XRD peaks reveals that the ZnO NFs are polycrystalline, and the dominance of the (002) peak in the XRD pattern indicates that the longitudinal direction of the ZnO NFs is largely perpendicular to the c-axis of the ZnO-lattice structure. These peaks are absent from the XRD pattern that is derived from the as-electrospun NFs, and they support the TG and DTA analyses that suggest that the synthesis and sintering of the ZnO grains occurs during the subsequent heating time; that is, the sintering time.

The dependences of the Seebeck coefficient and the electrical conductivity on the sintering time with respect to the NFs are examined in this study. The Seebeck coefficient and the electrical conductivity are plotted in Fig. 3 as a function of the sintering time; here, the Seebeck coefficient increases with the elapsed sintering time up to 30 min, but it decreases with the sintering time in the range from 30 min to 120 min. The maximum Seebeck coefficient of the NFs that were sintered for 30 min is -132.1 μV/K, while the Seebeck coefficient of the NFs that were sintered for 120 min is relatively much lower at - 44.6 μV/K. Differing from the decrease of the Seebeck coefficient, the electrical conductivity increased with the elapsed sintering time across the entire range of this study; that is, its magnitude increased from 2.07×10^{-3} S/m to 0.18 S/m. For the thermally treated NFs with sintering times that are shorter and longer than 30 min, the relationships of the Seebeck coefficients and the electrical conductivities are different from each other; the shorter and longer sintering regions are labeled region I and region II, respectively, in Fig. 3. The largely proportional relationship between the Seebeck coefficient and the electrical conductivity in region I demonstrates the transformation of the insulating NFs (made of the zinc-acetate dehydrate and polyvinyl pyrrolidone) into semiconducting NFs in that region. The inverse relationship between the Seebeck coefficient and the electrical conductivity in region II is

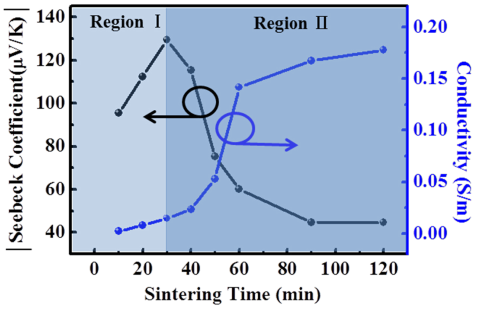

Fig. 3. Seebeck coefficient and electrical conductivity of the NFs as a function of the sintering time.

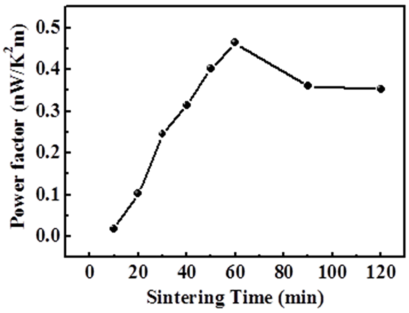

Fig. 5. Power factor (PF) as a function of the sintering time.

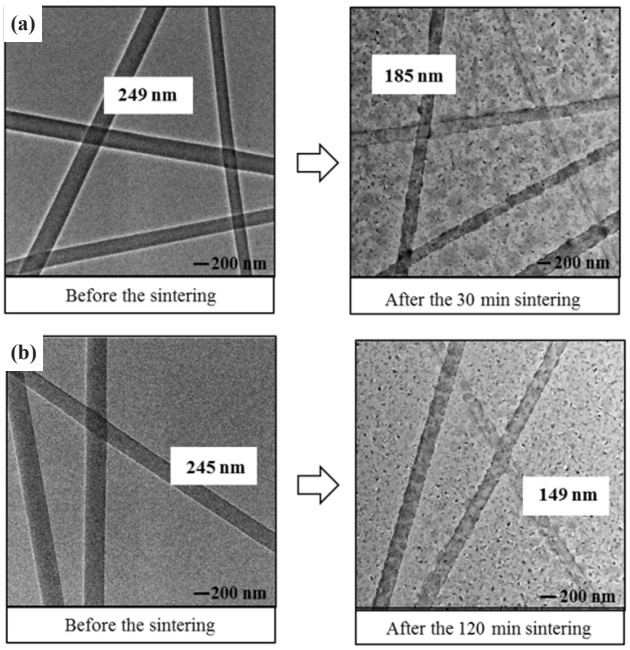

Fig. 4. HR-TEM images of the two selected NFs before and after sintering for (a) 30 min and (b) 120 min.

consistent with the thermoelectric characteristics of *n*-type ZnO-semiconducting materials [12].

A main reason for both the increase of the electrical conductivity and the decrease of the Seebeck coefficient is the shrinkage of the ZnO NFs. The compositional NF materials are solidified so that they are compact during the sintering, and the diameters are thereby reduced. The reduction of the diameters of the two selected ZnO NFs in accordance with the elapsed sintering time is demonstrated in Fig. 4. For one as-electrospun NF, the diameter is reduced from 249 nm to 185 nm after the sintering for 30 min, and for the other as-electrospun NF, the diameter shrinks from 245 nm to 149 nm after the sintering for 120 min.

The diameter reduction is more significant for the longer sintering time, thereby revealing that the compaction proceeds with the sintering. The smaller diameter comprises a greater compaction of the compositional materials inside the NFs, and the higher compaction leads to an improved transport of the charge carriers in the NFs [13,14]; simultaneously, the diameter contraction enhances the charge-carrier concentration. The electrical conductivity is therefore inversely related to the diameter; meanwhile, the enhancement of the charge-carrier concentration causes a decrease of the Seebeck coefficient [15]. The higher compaction of the compositional materials inside the NFs is therefore responsible for both the enhancement of the electrical conductivity and the diminishment of the Seebeck coefficient with the sintering (as shown in Fig. 3).

The power factor (PF) is a measure for the evaluation of the thermoelectric capability of the ZnO NFs. The PF is expressed as PF = S2σ, where S and σ are the Seebeck coefficient and the conductivity, respectively. The estimated PF values are plotted in Fig. 5 as a function of the sintering time. The plot shows that the maximum PF of the ZnO NFs that were sintered for 60 min is 0.46 nW/K2m; therefore, to enhance the thermoelectric capability, the sintering time should be optimized because of the trade-off relationship between the Seebeck coefficient and the electrical conductivity.

4. CONCLUSIONS

The effect of a thermal treatment on the thermoelectric characteristics of electrospinning-prepared NFs was investigated in this study; here, a heating time that is longer than 30 min at 550℃ enables the synthesis and the sintering of the *n*-type ZnO in the NFs. For the ZnO NFs, the Seebeck coefficient decreased from - 132.1 μV/K to - 44.6 μV/K with a heating-time decrease of 30 min to 120 min, while the electrical conductivity increased from 2.07×10^{-3} S/m to 0.18 S/m. The increase of the electrical conductivity and the decrease of the Seebeck coefficient with the sintering time originate from the thermal contraction of the diameters. Because of the trade-off relationship between the electrical conductivity and the Seebeck coefficient with respect to the sintering time, the maximum PF of the ZnO NFs that were sintered for 60 min is 0.46 nW/K2m. The present study demonstrates that the sintering time influences the thermoelectric characteristics of ZnO NFs through the thermal contraction of the diameters.

ACKNOWLEDGMENTS

This work was supported by the Mid-career Researcher Program (No. NRF-2013R1A2A1A03070750) that is funded by the Ministry of Education, Science and Technology through the National Research Foundation of Korea (NRF), and a National Research Foundation of Korea (NRF) Grant funded by the Korean Government (MSIP) (No. NRF-2015R1A5A7037674).

REFERENCES

[1] H. Wu, R. Zhang, X. Liu, D. Lin, and W. Pan, *Chem. Mater.*, **19**, 3506 (2007). [DOI: http://dx.doi.org/10.1021/cm070280i]

[2] H. Wu and W. Pan, *J. Am. Ceram. Soc.*, **89**, 699 (2006). [DOI: http://dx.doi.org/10.1111/j.1551-2916.2005.00735.x]

[3] F. Ma, Y. Ou, Y. Yang, Y. Liu, S. Xie, J. F. Li, G. Cao, R. Proksch, and J. Li, *J. Phys. Chem. C*, **114**, 22038 (2010). [DOI: http://dx.doi.org/10.1021/jp107488k]

[4] Z. M. Huanga, Y. Z. Zhang, M. Kotaki, and S. Ramakrishna, *Compos. Sci. Technol.*, **63**, 2223 (2003). [DOI: http://dx.doi.org/10.1016/S0266-3538(03)00178-7]

[5] M. Zhang, H. Park, J. Kim, H. Park, T. Wu, S. Kim, S. D. Park, Y. Choa, and N. V. Myung, *Chem. Mater.*, **27**, 5189 (2015). [DOI: http://dx.doi.org/10.1021/acs.chemmater.5b00960]

[6] S. Kocyigit, A. Aytimur, E. Cinar, I. Uslu, A. Akdemir, *JOM*, **66**, 30 (2014). [DOI: http://dx.doi.org/10.1007/s11837-013-0822-x]

[7] D. Lee, K. Cho, J. Choi, and S. Kim, *Mater. Lett.*, **142**, 250 (2015). [DOI: http://dx.doi.org/10.1016/j.matlet.2014.12.029]

[8] T. Yin, D. Liu, Y. Ou, F. Ma, S. Xie, J. F. Li, and J. Li, *J. Phys. Chem. C*, **114**, 10061 (2010). [DOI: http://dx.doi.org/10.1021/jp1024872]

[9] S. Maensiri and W. Nuansing, *Mater. Chem. Phys.*, **99**, 104 (2006). [DOI: http://dx.doi.org/10.1016/j.matchemphys.2005.10.004]

[10] W. Xu, Y. Shi, and H. Hadim, *Nanotechnology*, **21**, 395303 (2010). [DOI: http://dx.doi.org/10.1088/0957-4484/21/39/395303]

[11] S. S. Mali, H. Kim, W. Y. Jang, H. S. Park, P. S. Patil, and C. K. Hong, *ACS Sustainable Chem. Eng.*, **1**, 1207 (2013). [DOI: http://dx.doi.org/10.1021/sc400153j]

[12] R. Koc and H. U. Anderson, *J. Mater. Sci.*, **27**, 5477 (1992). [DOI: http://dx.doi.org/10.1007/BF00541609]

[13] A. Laforgue and L. Robitaille, *Synth. Met.*, **158**, 577 (2008). [DOI: http://dx.doi.org/10.1016/j.synthmet.2008.04.004]

[14] I. D. Norris, M. M. Shaker, F. K. Ko, and A. G. MacDiarmid, *Synth. Met.*, **144**, 109 (2000). [DOI: http://dx.doi.org/10.1016/S0379-6779(00)00217-4]

[15] N. Mateeva, H. Niculescu, J. Schlenoff, and L. R. Testardi, *J. Appl. Phys.*, **83**, 3111 (1998). [DOI: http://dx.doi.org/10.1063/1.367119]